

# GUIDANCE, NAVIGATION AND ATTITUDE CONTROL OF MINI-SATELLITES IN A LOW EARTH ORBIT CONSTELLATION FOR AREAL SURVEY

**Yevgeny Somov<sup>1,2</sup>**

<sup>1</sup>Navigation, Guidance and Control  
Samara State Technical University

<sup>2</sup>Dynamics and Motion Control  
Samara Federal Research  
Scientific Center RAS

Samara, Russia  
e\_somov@mail.ru

**Sergey Butyrin<sup>1,2</sup>**

<sup>1</sup>Navigation, Guidance and Control  
Samara State Technical University

<sup>2</sup>Dynamics and Motion Control  
Samara Federal Research  
Scientific Center RAS

Samara, Russia  
butyrinsa@mail.ru

**Sergey Somov<sup>1,2</sup>**

<sup>1</sup>Navigation, Guidance and Control  
Samara State Technical University

<sup>2</sup>Dynamics and Motion Control  
Samara Federal Research  
Scientific Center RAS

Samara, Russia  
s\_somov@mail.ru

Article history:

Received 15.05.2023, Accepted 15.09.2023

## Abstract

The problems of guidance, navigation and attitude control in a constellation of mini-observation satellites are considered. The developed methods and algorithms for scanning areal survey performed by these constellations in the low sun-synchronous orbits are presented.

The most important new results are methods for coordinated angular guidance of satellites in the constellation's orbital planes and the comparison results for sequences of the areal space surveys.

## Key words

Satellite constellation, areal Earth survey, guidance, navigation and attitude control.

## Abbreviations

AOCS	=	Attitude and Orbit Control System
BRF	=	Body Reference Frame
FRF	=	Field Reference Frame
GD	=	Gyrodine
GMC	=	Gyro Moment Cluster
GRF	=	Greenwich Reference Frame
HRF	=	Horizon Reference Frame
IMU	=	Inertial Measurement Unit
IMV	=	Image Motion Velocity
IRF	=	Inertial Reference Frame
OEC	=	Optoelectronic Converter
ORF	=	Orbital Reference Frame
SR	=	Scanning Route
SRF	=	Sensor Reference Frame
STC	=	Star Tracker Cluster
TM	=	Turning Maneuver

## 1 Introduction

Problems of guidance, navigation and motion control are relevant for all modern spacecraft (SC) [Aleksandrov and Tikhonov, 2018; Somov et al., 2021a], including the space optoelectronic systems for Earth surveying [Somov et al., 2022].

The observation mini-satellites have a mass of up to 500 kg and their structure contains large-size solar array panels for a power-supplying of the satellite equipment, including attitude and orbit control system (AOCS), which has strapdown inertial navigation system (SINS) with inertial measurement unit (IMU) based on gyro sensors corrected by signals of navigation satellites and star tracker cluster (STC).

The operation of mini-satellites in low Earth orbit has several advantages in both SC design and its mission objectives. Implementing such satellites has been proposed as a means to reduce both the cost of satellite development and launch as well as to obtain higher spatial resolution imagery. Modern research, developments and the latest problem issues on this topic were previously presented in [Crisp et al., 2021] with 97 items in the list of related publications. Here, the problems of AOCSs are discussed for both optoelectronic and synthetic aperture radar satellites, including advanced observation SC based on new technologies.

The requirements for AOCS of an Earth-surveying SC are as follows: (i) guidance of the telescope's line-of-sight to a predetermined part of the Earth surface with a scanning route (SR) in a designated direction; (ii) stabilization of an image motion velocity (IMV) in a telescope focal plane. Attitude guidance laws of such a

satellite are presented by a sequence of the time intervals for the observing SRs and turning maneuvers (TMs) [Somov et al., 2018]. Lifetime up to 10 years, fast spatial TMs with effective damping the SC structure oscillations as well as reasonable mass, size and energy characteristics have the motivated development of AOCSS equipped with gyro moment clusters (GMCs) based on gyrodines (GDs) – single-gimbal control moment gyroscopes. Many studies have been carried out on the orbital structures of information satellites [Ballard, 1980; Walker, 1984; Mozhaev, 1989; Lang, 2003; Chernov and Chernyavsky, 2004; Ulybyshev, 2016; Razoumny, 2016; Ulybyshev and Lysenko, 2019], including constellations of Earth-observing mini-satellites [Rodriguez-Donaire and et al., 2020; Lappas and Kostopoulos, 2020].

The article briefly presents results on guidance, navigation and control in mini-satellite constellations during a scanning areal optoelectronic survey. Here, for the first time we are solving the problem of analytical synthesis of the SC angular guidance laws during areal surveying, when the CCD matrix in the telescope's focal plane has a reverse mode. The developed methods for coordinated guidance of mini-satellites in the orbital planes of a constellation as well as the comparison results of various sequences in areal space surveys are new and original. In seven sections of the article, we present the full range of results – beginning from math modeling to simulation.

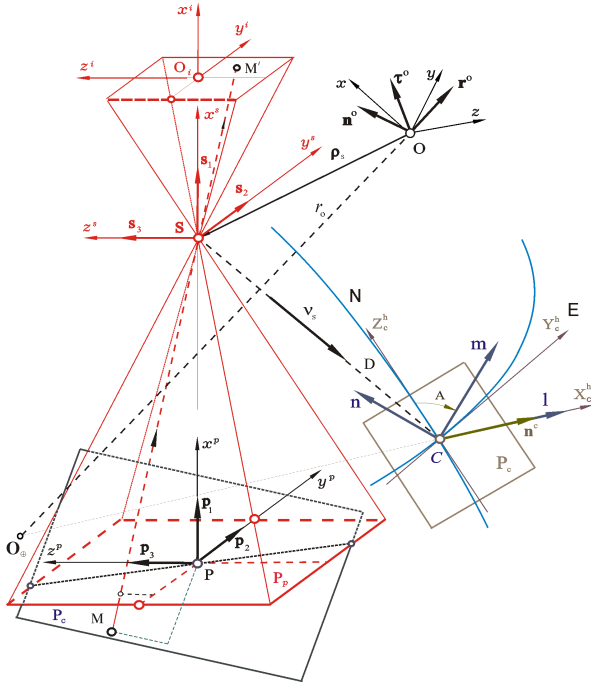


Figure 1. The reference frames for a space Earth survey

## 2 Models and the Problem Statement

The following reference frames are introduced: inertial sun-ecliptic reference frame  $O_{\odot} X_s^I Y_s^I Z_s^I$ ; inertial reference frame (IRF)  $O_{\oplus} X_e^I Y_e^I Z_e^I$  with the origin  $O_{\oplus}$ ; geodesic Greenwich reference frame (GRF)  $O_{\oplus} X^e Y^e Z^e$  rotated in IRF by angular velocity vector  $\omega_{\oplus}$ ; geodesic

horizon reference frame (HRF)  $C X_c^h Y_c^h Z_c^h$  with the origin in point  $C$  and ellipsoidal coordinates – altitude  $H_c$ , longitude  $L_c$  and latitude  $B_c$ , axis  $C X_c^h$  is local vertical, axes  $C Y_c^h$  and  $C Z_c^h$  lie in the local horizon plane and directed to local East (E) and local North (N), Fig. 1; the SC body reference frame (BRF)  $Ox y z$  and orbit reference frame (ORF)  $Ox^o y^o z^o$  with the origin in the SC mass center  $O$ ; the telescope (sensor) reference frame (SRF)  $Sx^s y^s z^s$  with the origin in point  $S$  – center of optical projection; the image field reference frame (FRF)  $O_i x^i y^i z^i$  with the origin in center  $O_i$  of the telescope focal plane  $y^i O_i z^i$ ; visual (sighting) reference frame (VRF)  $O_v x^v y^v z^v$  with the origin in center  $O_v$  of the CCD array, Figs. 1 and 2.

We introduce also the virtual bases G and A which are computed by processing the measuring information respectively from the IMU and STC. For simplicity we will propose that the bases **B** and **S** (BRF and SRF) coincide.

In the IRF  $\mathbf{I} \equiv \mathbf{I}_{\oplus}$  the BRF orientation is defined by quaternion  $\mathbf{\Lambda}_I^b \equiv \mathbf{\Lambda} = (\lambda_0, \boldsymbol{\lambda})$ ,  $\boldsymbol{\lambda} = \{\lambda_1, \lambda_2, \lambda_3\}$  and with respect to ORF – by column  $\boldsymbol{\phi} = \{\phi_i\}$ ,  $i = 1, 2, 3 \equiv 1 \div 3$  of Euler-Krylov angles  $\phi_1$  (roll),  $\phi_2$  (yaw) and  $\phi_3$  (pitch).

We apply also vector of the modified Rodrigues parameters (MRP)  $\boldsymbol{\sigma} = \{\sigma_i\} = \mathbf{e} \tan(\Phi/4)$  with Euler unit vector  $\mathbf{e}$  and angle  $\Phi$  of own rotation. Vector  $\boldsymbol{\sigma}$  is one-one connected with quaternion  $\mathbf{\Lambda}$  by explicit relations.

We use notation  $\boldsymbol{\omega}(t)$ ,  $\mathbf{r}(t)$  and  $\mathbf{v}(t)$  for vectors of the SC body angular velocity, its mass center's position and progressive velocity in the IRF as well as symbols  $\langle \cdot, \cdot \rangle$ ,  $\{ \cdot \}$ ,  $[ \cdot ] = \text{line}(\cdot)$  for vectors and  $[ \cdot \times ]$ ,  $( \cdot )^t$  for matrices.

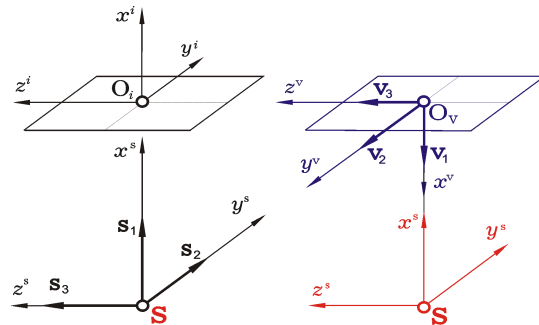


Figure 2. The telescope reference frames

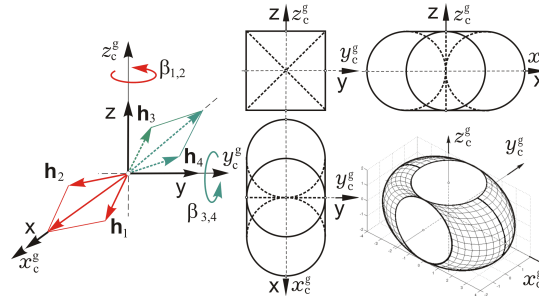


Figure 3. The GMC scheme 2-SPE based on four GDs

Collinear pair GDs was named as *Scissored Pair Ensemble (SPE)*. Column  $\mathbf{H}(\boldsymbol{\beta}) \equiv \mathbf{h}_g \mathbf{h}(\boldsymbol{\beta}) = \mathbf{h}_g \boldsymbol{\Sigma} \mathbf{h}_p(\boldsymbol{\beta}_p)$

with vectors  $\beta \equiv \{\beta_p\}$  and  $\mathbf{h}(\beta) \in \mathcal{S} \subset \mathbb{R}^3$  presents the angular momentum (AM) vector of the GMC by scheme 2-SPE based on 4 GDs, where  $\mathbf{h}_g$  is a constant own AM of each GD. Figure 3 presents simplest arrangement of this scheme with  $|\mathbf{h}_p|=1 \forall p=1 \div 4$ , which in park state has the vector of normed AM  $\mathbf{h}(\beta)=\mathbf{0}$ . For a fixed position of the SC flexible structures and  $t \in T_{t_0}=[t_0, +\infty)$  the SC angular motion model is appeared as follows

$$\dot{\mathbf{A}} = \mathbf{A} \circ \boldsymbol{\omega} / 2; \quad \mathbf{A}^o \{\dot{\boldsymbol{\omega}}, \dot{\mathbf{q}}\} = \{\mathbf{F}^\omega, \mathbf{F}^q\}, \quad (1)$$

$\boldsymbol{\omega} = \{\omega_i, i=x, y, z \equiv 1 \div 3\}; \mathbf{q} = \{q_j, j=1 \div n^q\};$   
 $\mathbf{F}^\omega = \mathbf{M}^g - \boldsymbol{\omega} \times \mathbf{G} + \mathbf{M}^d(t, \mathbf{A}, \boldsymbol{\omega}) + \mathbf{Q}^o(\boldsymbol{\omega}, \dot{\mathbf{q}}, \mathbf{q});$   
 $\mathbf{F}^q = \{-a_j^q((\delta^q/\pi)\Omega_j^q \dot{q}_j + (\Omega_j^q)^2 q_j) + Q_j^q(\boldsymbol{\omega}, \dot{q}_j, q_j)\};$   
 $\mathbf{A}^o = \begin{bmatrix} \mathbf{J} & \mathbf{D}_q \\ \mathbf{D}_q^t & \mathbf{A}^q \end{bmatrix}; \mathbf{G} = \mathbf{G}^o + \mathbf{D}_q \dot{\mathbf{q}}; \mathbf{M}^g = -\mathbf{h}_g \mathbf{A}_h(\beta) \dot{\beta};$   
 vector  $\mathbf{M}^d(\cdot)$  presents the external disturbance torques, and  $\mathbf{Q}^o(\cdot)$ ,  $Q_j^q(\cdot)$  are nonlinear continuous functions. Vector  $\mathbf{M}^g = \{\mathbf{M}_i^g\}$  of the GMC control torque is represented by the nonlinear relations

$\mathbf{M}^g = -\mathcal{H}' = -\mathbf{h}_g \mathbf{A}_h(\beta) \mathbf{u}_k^g(t); \dot{\beta} = \mathbf{u}_k^g(t) \equiv \{u_{pk}^g(t)\}$   
 with control  $u_{pk}^g(t) = \text{Zh}[\text{sat}(\text{qntz}(u_{pk}^g, u_g^o), u_g^m), T_u]$ ,  $k \in \mathbb{N}_0$ , a period  $T_u$  and symbol  $(\cdot)'$  of local time derivative. Singular state of 2-SPE scheme is appeared if Gram matrix  $\mathbf{G}(\beta) = \mathbf{A}_h(\beta) \mathbf{A}_h^t(\beta)$  loses its full rang, i.e. when  $\mathbf{G}(\beta) \equiv \det \mathbf{G}(\beta) = 0$ . At given the SC body angular guidance law  $\mathbf{A}^p(t), \boldsymbol{\omega}^p(t), \boldsymbol{\varepsilon}^p(t) = \dot{\boldsymbol{\omega}}^p(t)$  during a time  $t \in T \equiv [t_i, t_f] \subset T_{t_0}$ ,  $t_f \equiv t_i + T$  when forming the GMC control torque vector  $\mathbf{M}^g$ , the columns  $\dot{\beta} = \{\dot{\beta}_p\}$  and  $\ddot{\beta} = \{\ddot{\beta}_p\}$  have modular-restricted components:  $|\dot{\beta}_p(t)| \leq \bar{u}_g < \bar{u}_g^m, |\ddot{\beta}_p(t)| \leq \bar{v}_g, \forall t \in T$  with given positive constants  $\bar{u}_g$  and  $\bar{v}_g$ .

At simplest modeling of the SC body with a fixed telescope as a free solid, its AM vector is  $\mathbf{G}^o \equiv \mathbf{0}$  when the satellite ACS is balanced on the AM. Moreover, the model of the SC attitude dynamics has the form  $\dot{\boldsymbol{\omega}} = \boldsymbol{\varepsilon}$ , where  $\boldsymbol{\varepsilon} = \mathbf{J}^{-1} \mathbf{M}^g$  is vector of angular acceleration, and the model of SC attitude motion has the following kinematic representation

$$\dot{\mathbf{A}}(t) = \mathbf{A}(t) \circ \boldsymbol{\omega}(t) / 2; \dot{\boldsymbol{\omega}}(t) = \boldsymbol{\varepsilon}(t); \dot{\boldsymbol{\varepsilon}}(t) \equiv \boldsymbol{\varepsilon}'(t) = \mathbf{v}. \quad (2)$$

Modules of vectors  $\boldsymbol{\omega}(t)$ ,  $\boldsymbol{\varepsilon}(t)$  and  $\dot{\boldsymbol{\varepsilon}}(t)$  are restricted,  $|\boldsymbol{\omega}(t)| \leq \bar{\omega}$ ,  $|\boldsymbol{\varepsilon}(t)| \leq \bar{\varepsilon}$  and  $|\dot{\boldsymbol{\varepsilon}}(t)| \leq \bar{\varepsilon}'$ , that is connected with a limited envelop of the variation domains for vectors of the GMC angular momentum  $\mathcal{H}$  and control torque  $\mathbf{M}^g$  with permissible velocity of its variation.

Principal problems get up on a planning the space land-survey and the SC angular guidance at its route motion when a space observation is executed at given time interval  $t \in T$  – determination of quaternion  $\mathbf{A}^p(t)$ , vectors  $\boldsymbol{\omega}^p(t)$  and  $\boldsymbol{\varepsilon}^p(t)$  in the form of explicit time functions, proceed from the main requirement: optical image of the Earth given part must move by desired way at the telescope focal plane.

Assume that for any time interval  $T$  the SC attitude guidance law was obtained as data in points  $t_l \in T$ ,  $l \in \bar{\mathbb{N}} \subset \mathbb{N}_0$  by integrating the quaternion equation in (2). This law corresponds to required SR by arbitrary type – trace, orthodromic, with optimal equalization of

a longitudinal IMV, stereo observation et al. The problem consists in analytical representation of the guidance law  $\mathbf{A}^p(t), \boldsymbol{\omega}^p(t)$  without any restriction on duration of interval  $T$ . If we have two adjacent SRs, then for the satellite TM we have obtained the boundary conditions by quaternion, vectors  $\boldsymbol{\omega}$  and  $\boldsymbol{\varepsilon}$  and in general case also by the vector  $\dot{\boldsymbol{\varepsilon}}$  in a time moment when the second SR is beginning. For the TM time interval  $t \in T_p^r \equiv [t_1^p, t_f^p]$ ,  $t_f^p \equiv t_1^p + T_p^r$  and the general boundary conditions

$$\begin{aligned} \mathbf{A}(t_1^p) &= \mathbf{A}_i; \boldsymbol{\omega}(t_1^p) = \boldsymbol{\omega}_i; \boldsymbol{\varepsilon}(t_1^p) = \boldsymbol{\varepsilon}_i; \\ \mathbf{A}(t_f^p) &= \mathbf{A}_f; \boldsymbol{\omega}(t_f^p) = \boldsymbol{\omega}_f; \boldsymbol{\varepsilon}(t_f^p) = \boldsymbol{\varepsilon}_f; \dot{\boldsymbol{\varepsilon}}(t_f^p) = \dot{\boldsymbol{\varepsilon}}_f \end{aligned} \quad (3)$$

taking into account given restrictions on vectors  $\boldsymbol{\omega}(t)$  and  $\boldsymbol{\varepsilon}(t)$  we consider the problem on synthesis of a guidance law at the spacecraft TM using analytic relations only.

The problems of the SINS signal processing are connected with integration of kinematic equations in using the information only on the increment vector

$\mathbf{i}_{ms}^{g\omega} = \text{Int}(t_s, T_q, \boldsymbol{\omega}_m^g(\tau)) + \boldsymbol{\delta}_s^n$ ;  $\mathbf{A}_{mnr}^a = \mathbf{A}_r \circ \mathbf{A}_r^n$ ;  $s \in \mathbb{N}_0$   
 with measured vector  $\boldsymbol{\omega}_m^g(t) \equiv (1+m)\mathbf{S}^\Delta(\boldsymbol{\omega}(t) + \mathbf{b}^g)$  [Somov et al., 2019] at the period  $T_q \ll T_o$  obtained by the IMU at availability of noises, calibration (identification of the IMU bias  $\mathbf{b}^g$  and variation of the measure scale factor  $m$ ) and alignment (identification mutual position of the STC with both a telescope and the IMU) by STC signals only in the time moment  $t_r$ ,  $r \in \mathbb{N}_0$  with the period  $T_o$ . During a lifetime up to 10 years the mini-satellite structure characteristics are slowly changed in wide boundaries, solar array panels are rotated and communications antennas are pointing for information service. General problem consists in dynamical designing the GMC's robust digital control law  $\mathbf{u}_k^g = \{u_{pk}^g\}$ .

### 3 Planning of Areal Survey

The aim of an areal survey is to cover a given area on

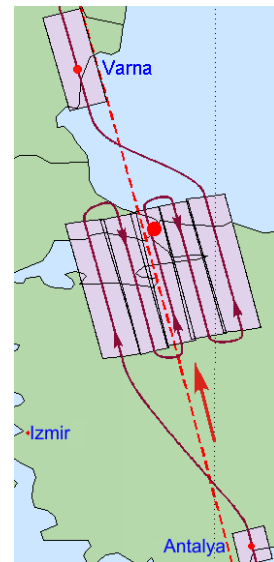


Figure 4. The scheme of Earth areal survey

the Earth's surface with geographical center  $C$  by a sequence of partly overlapping scanning routes (OSRs).

Assume that optoelectronic converters (OECs) in the telescope focal plane have the reverse mode. The initial data for planning such a land-survey are the size of the area  $S = a \times b$  with length  $a$  and width  $b$ , parameters of the SC spatial motion, characteristics of the telescope and OECs. Figure 4 represents the map with projections of scans and the telescope target line trace obtained in planning the areal land-surveying neighborhoods of Istanbul by a small SC in sun-synchronous orbit with altitude of 720 km [Somov et al., 2019] when the allowed deviation of the target line from Nadir is within the cone with semi-angle of 30 deg.

#### 4 The Satellite Guidance Laws

Analytic matching solution have been obtained for problem of the SC guidance during any scanning route. The solution is based on a vector composition of all motions in GRF using the reference frames HRF, SRF and FRF. For any observed point  $C$  the oblique range  $D$  is analytically calculated as  $D = |\mathbf{r}_c^e - \mathbf{r}^e|$ . If matrix  $\mathbf{C}_h^s \equiv \tilde{\mathbf{C}} = \|\tilde{c}_{ij}\|$  defines the SRF orientation in HRF  $\mathbf{E}_e^h$ , then for any point  $M(\tilde{y}^i, \tilde{z}^i)$  in the telescope focal plane, Fig. 1, the components  $\tilde{V}_y^i$  and  $\tilde{V}_z^i$  of the IMV normed vector are computed as follows

$$\begin{bmatrix} \tilde{V}_y^i \\ \tilde{V}_z^i \end{bmatrix} = \begin{bmatrix} \tilde{y}^i & 1 & 0 \\ \tilde{z}^i & 0 & 1 \end{bmatrix} \begin{bmatrix} q^i \tilde{v}_{e1}^s - \tilde{y}^i \omega_{e3}^s + \tilde{z}^i \omega_{e2}^s \\ q^i \tilde{v}_{e2}^s - \omega_{e3}^s - \tilde{z}^i \omega_{e1}^s \\ q^i \tilde{v}_{e3}^s + \omega_{e2}^s + \tilde{y}^i \omega_{e1}^s \end{bmatrix}. \quad (4)$$

Here  $\tilde{y}^i = y^i/f_e$ ,  $\tilde{z}^i = z^i/f_e$  are normed focal coordinates where function  $q^i \equiv 1 - (\tilde{c}_{21}\tilde{y}^i + \tilde{c}_{31}\tilde{z}^i)/\tilde{c}_{11}$ , and vector of normed SC mass center velocity has the components  $\tilde{v}_{ei}^s = v_{ei}^s/D$ ,  $i = 1 \div 3$ . The ratio (4) combines the SC motion control and signal processing in optoelectronics [Somov et al., 2022], i.e. in cybernetics and physics.

Let us consider a time interval  $T \equiv [0, T]$  with the following notation for its four points  $\tau_p$ ,  $p = 1 \div 4$  :  $\tau_1 = 0$ ,  $\tau_2 = T/3$ ,  $\tau_3 = 2T/3$  and  $\tau_4 = T$ . For six values  $\boldsymbol{\omega}_l = \boldsymbol{\omega}(t_l)$  nearby points  $\tau_1 = 0$ ,  $\tau_4 = T$  standard interpolation is carried out by the vector spline of degree five. This allows us to calculate values  $\boldsymbol{\varepsilon}_1 = \dot{\boldsymbol{\omega}}(\tau_1)$  and  $\boldsymbol{\varepsilon}_4 = \dot{\boldsymbol{\omega}}(\tau_4)$  of angular acceleration vector. For four points  $\tau_p \in T$  values  $\boldsymbol{\sigma}_p$ ,  $p = 1 \div 4$  are computed, also values  $\dot{\boldsymbol{\sigma}}_p$  and  $\ddot{\boldsymbol{\sigma}}_p$ ,  $p = 1, 4$  for two boundary points. Interpolation of the MRP vector  $\boldsymbol{\sigma}(t) \forall t \in T$  is carried out by the vector spline of 7 degree  $\boldsymbol{\sigma}_a(t) = \sum_0^7 \mathbf{a}_s t^s$  with 8 columns  $\mathbf{a}_s \in \mathbb{R}^3$ ,  $s = 0 \div 7$  of coefficients.

Eight columns  $\mathbf{a}_s$  are defined for spline  $\boldsymbol{\sigma}_a(t)$  on the basis of (i) three boundary conditions  $\boldsymbol{\sigma}_a(0) = \boldsymbol{\sigma}_1$ ;  $\dot{\boldsymbol{\sigma}}_a(0) = \dot{\boldsymbol{\sigma}}_1$ ;  $\ddot{\boldsymbol{\sigma}}_a(0) = \ddot{\boldsymbol{\sigma}}_1$  on the left end of interval  $T$ , which results in  $\mathbf{a}_0 = \boldsymbol{\sigma}_1$ ,  $\mathbf{a}_1 = \dot{\boldsymbol{\sigma}}_1$  and  $\mathbf{a}_2 = \ddot{\boldsymbol{\sigma}}_1/2$ ; (ii) two conditions  $\boldsymbol{\sigma}_a(\tau_2) = \boldsymbol{\sigma}_2$ ;  $\boldsymbol{\sigma}_a(\tau_3) = \boldsymbol{\sigma}_3$  in points  $\tau_2$  and  $\tau_3$ ; (iii) three boundary conditions  $\boldsymbol{\sigma}_a(T) = \boldsymbol{\sigma}_4$ ;  $\dot{\boldsymbol{\sigma}}_a(T) = \dot{\boldsymbol{\sigma}}_4$ ;  $\ddot{\boldsymbol{\sigma}}_a(T) = \ddot{\boldsymbol{\sigma}}_4$ . Elaborated matrix relation is applied for simultaneous analytical computation of all five sought columns  $\mathbf{a}_s$ ,  $s = 3 \div 7$  [Somova, 2016].

For SC turning maneuver on a time interval  $T_p^r$  with the general boundary conditions (3) we have developed analytical method for synthesis of the SC angular guid-

ance law based on the necessary and sufficient condition for solvability of Darboux problem. The solution is presented as the result of composition three simultaneously derived rotations of "embedded" bases  $\mathbf{E}_k$  about the unit vectors  $\mathbf{e}_k$ ,  $k = 1 \div 3$  of Euler axes, when  $\boldsymbol{\Lambda}$  is defined as  $\boldsymbol{\Lambda}(t) = \boldsymbol{\Lambda}_1 \circ \boldsymbol{\Lambda}_1(t) \circ \boldsymbol{\Lambda}_2(t) \circ \boldsymbol{\Lambda}_3(t)$ , where  $\boldsymbol{\Lambda}_k(t) = (\cos(\varphi_k(t)/2), \mathbf{e}_k \sin(\varphi_k(t)/2))$ .

Let us the quaternion  $\boldsymbol{\Lambda}^* \equiv (\lambda_0^*, \boldsymbol{\lambda}^*) = \tilde{\boldsymbol{\Lambda}}_i \circ \boldsymbol{\Lambda}_f$  has unit vector  $\mathbf{e}_3 = \boldsymbol{\lambda}^*/\sin(\varphi^*/2)$  of 3rd rotation with angle  $\varphi^* = 2 \arccos(\lambda_0^*)$ . For quaternions  $\boldsymbol{\Lambda}_k$  the boundary conditions  $\boldsymbol{\Lambda}_1(t_f^p) = \boldsymbol{\Lambda}_1(t_f^p) = \boldsymbol{\Lambda}_2(t_f^p) = \boldsymbol{\Lambda}_2(t_f^p) = \mathbf{1}$ ;  $\boldsymbol{\Lambda}_3(t_f^p) = \mathbf{1}$ ,  $\boldsymbol{\Lambda}_3(t_f^p) = (\cos(\varphi_3^f/2), \mathbf{e}_3 \sin(\varphi_3^f/2))$  are applied, where  $\varphi_3^f = \varphi^*$  and  $\mathbf{1}$  is unit quaternion.

We use notation  $\boldsymbol{\omega}^{(k)}, \boldsymbol{\varepsilon}^{(k)}, \dot{\boldsymbol{\varepsilon}}^{(k)}$  with  $k = 1 \div 3$  for vectors  $\boldsymbol{\omega}$ ,  $\boldsymbol{\varepsilon}$  and  $\dot{\boldsymbol{\varepsilon}}$  in basis  $\mathbf{E}_k$ , the operator  $\mathbf{a}^{(k)} = \Phi(\mathbf{a}^{(k-1)}) \equiv \tilde{\boldsymbol{\Lambda}}_k \circ \mathbf{a}^{(k-1)} \circ \boldsymbol{\Lambda}_k$  for transforming the vector  $\mathbf{a}$  from basis  $\mathbf{E}_{k-1}$  to basis  $\mathbf{E}_k$ , and also notation  $\boldsymbol{\omega}_{k-1}^{(k)} = \Phi(\boldsymbol{\omega}_{k-1})$ ;  $\boldsymbol{\varepsilon}_{k-1}^{(k)} = \Phi(\boldsymbol{\varepsilon}_{k-1})$ ,  $\dot{\boldsymbol{\varepsilon}}_{k-1}^{(k)} = \Phi(\dot{\boldsymbol{\varepsilon}}_{k-1})$ . If we assign the vectors  $\boldsymbol{\omega}_1 = \dot{\varphi}_1(t)\mathbf{e}_1$ ,  $\boldsymbol{\varepsilon}_1 = \ddot{\varphi}_1(t)\mathbf{e}_1$  and  $\dot{\boldsymbol{\varepsilon}}_1 = \ddot{\varphi}_1(t)\mathbf{e}_1$ , then vectors  $\boldsymbol{\omega}(t)$ ,  $\boldsymbol{\varepsilon}(t)$  and  $\dot{\boldsymbol{\varepsilon}}(t)$  are computed by recurrent formulas with superscript  $k = 2, 3$ :

$$\begin{aligned} \boldsymbol{\omega}^{(k)} &= \boldsymbol{\omega}_{k-1}^{(k)} + \boldsymbol{\omega}_k; & \boldsymbol{\varepsilon}^{(k)} &= \boldsymbol{\varepsilon}_{k-1}^{(k)} + \boldsymbol{\varepsilon}_k + \boldsymbol{\omega}_{k-1}^{(k)} \times \boldsymbol{\omega}_k; \\ \dot{\boldsymbol{\varepsilon}}^{(k)} &= \dot{\boldsymbol{\varepsilon}}_{k-1}^{(k)} + \dot{\boldsymbol{\varepsilon}}_k + \boldsymbol{\omega}_{k-1}^{(k)} \times \boldsymbol{\varepsilon}_k + (2\boldsymbol{\varepsilon}_{k-1}^{(k)} + \boldsymbol{\omega}_{k-1}^{(k)} \times \boldsymbol{\omega}_k) \times \boldsymbol{\omega}_k. \end{aligned}$$

As a result, we obtain functions  $\boldsymbol{\omega}(t) = \boldsymbol{\omega}^{(3)}$ ,  $\boldsymbol{\varepsilon}(t) = \boldsymbol{\varepsilon}^{(3)}$  and  $\dot{\boldsymbol{\varepsilon}}(t) = \dot{\boldsymbol{\varepsilon}}^{(3)}$  by explicit analytic relations when assigning splines  $\varphi_k(t)$  by different degrees, in general case using three parts of given TM time interval  $T_p^r$ :

- (i) initial part of the under constraints when the SC moves to its angular motion on fixed unit vector  $\mathbf{e}_3$ ;
- (ii) the part for SC motion with a constant angular velocity on the unit vector  $\mathbf{e}_3$ ;
- (iii) the final part to guarantee the specified boundary conditions on the TM right end when the sixth order scalar splines  $\varphi_k(t)$  are applied.

All parameters of these splines are computed by explicit analytic relations and for sequence of the SRs and TMs we obtain the uniform vector spline attitude guidance law which is a command signal for the AOCS.

#### 5 The SINS Aligning and Calibration

Angular movements of a mini-satellite are performed on sequence of time intervals for the observation SRs

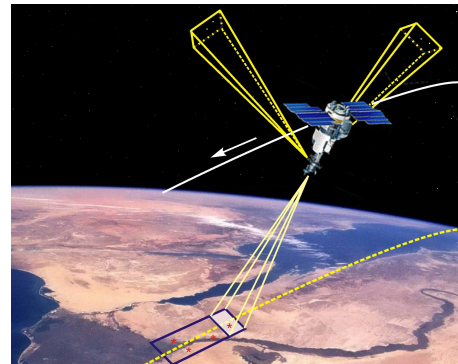


Figure 5. Aligning STC and telescope by the Earth marks

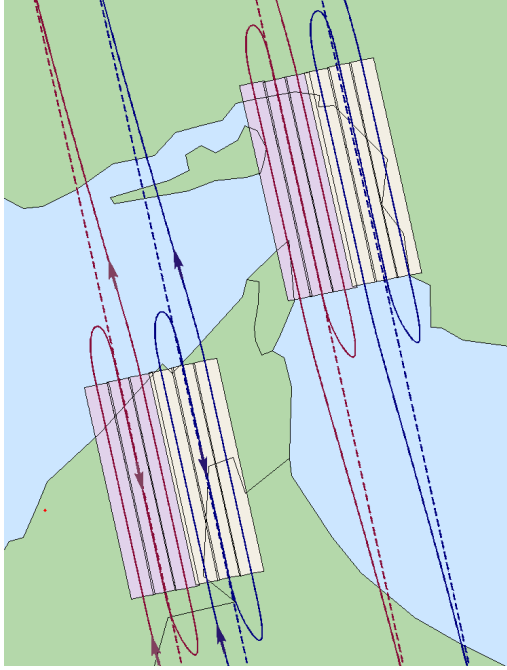


Figure 6. Areal scanning survey of the Hormuz Strait environs

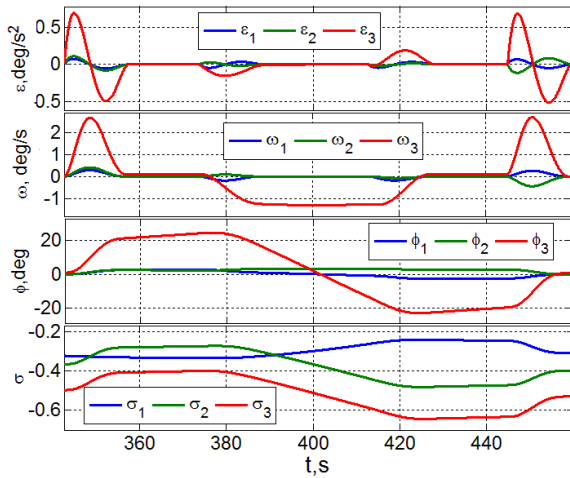


Figure 7. The angular guidance law for mini-satellite #1

and quick TMs with variable direction of angular velocity vector  $\omega$  when its module of up to value  $\omega^m = 3$  deg/s.

First, the telescope orientation is determined by the actual values  $\Lambda_r$  of its quaternion during scanning optoelectronic observation of terrestrial polygons with the reference marks, Fig. 5. In this mode, the SC fulfills a slow program movement, given by a set of splines for the MRP vector  $\sigma(t)$  when the AOCS operation.

The sequence of the telescope actual angular positions in the IRF is calculated by known method of backward dynamic photogrammetric serif with exact binding to the time moments  $t_r$ . At the same time moments, the STC orientation is measured in IRF, see Fig. 5, that makes it possible to calculate their mutual position using methods of optimal vector discrete filtering. The SINS alignment and calibration algorithms are based on the estimates  $\hat{\mathbf{b}}_r^g$ ,  $\hat{\mathbf{S}}_r^\Delta$  and  $\hat{m}_r$  during all modes of the SC attitude motion.

To compensate variations in the drift, scale and mutual position of the IMU and STC, the continuous vector estimation  $\hat{\mathbf{i}}_r^\omega(\tau)$  in basis A is computed by relation

$$\hat{\mathbf{i}}_r^\omega(\tau) = (1 - \hat{m}_r) (\hat{\mathbf{S}}_r^\Delta)^t (\hat{\mathbf{i}}_r^g(\tau) - \hat{\mathbf{b}}^g \tau), \quad \tau \in [t_r, t_{r+1}],$$

moreover  $\hat{\mathbf{i}}_{r+1}^\omega = \hat{\mathbf{i}}_r^\omega(T_o)$  [Somov et al., 2017].

## 6 Adaptive-Robust Attitude Control

At given the SC angular guidance law  $\Lambda^p(t)$ ,  $\omega^p(t)$ ,  $\epsilon^p(t)$  the error quaternion  $\mathbf{E} = (e_0, \mathbf{e}) = \tilde{\Lambda}^p \circ \Lambda$  with the vector  $\mathbf{e} = \{e_i\}$  corresponds to the attitude error matrix  $\mathbf{C}^e = \mathbf{I}_3 - 2[\mathbf{e} \times] \mathbf{Q}_e^t$  with  $\mathbf{Q}_e = \mathbf{I}_3 e_0 + [\mathbf{e} \times]$ , the angular error vector  $\delta\phi = \{\delta\phi_i\} = 2e_0 \mathbf{e}$ , and error in the angular velocity vector is defined as  $\delta\omega \equiv \{\delta\omega_i\} = \omega - \mathbf{C}^e \omega^p$ .

The vector  $\delta\phi_l \equiv \delta_l$  is discrete filtered with the period  $T_p$  and then values of mismatch vector  $\epsilon_k^f = -\delta_k^f \equiv -\{\delta_{ik}^f\}$  are applied in the GMC digital control law

$$\begin{aligned} \mathbf{g}_{k+1} &= \mathbf{B} \mathbf{g}_k + \mathbf{C} \epsilon_k^f; \quad \tilde{\mathbf{m}}_k = \mathbf{K}(\mathbf{g}_k + \mathbf{P} \epsilon_k^f); \\ \mathbf{M}_k^g &= \omega_k \times \mathbf{G}_k^o + \mathbf{J}(\mathbf{C}_k^e \epsilon_k^f + [\mathbf{C}_k^e \omega_k^p \times] \omega_k + \tilde{\mathbf{m}}_k), \end{aligned} \quad (5)$$

where for  $d_u \equiv 2/T_u$ ,  $a_i \equiv (d_u \tau_{1i} - 1)/(d_u \tau_{1i} + 1)$  elements of diagonal matrices  $\mathbf{K}$ ,  $\mathbf{B}$ ,  $\mathbf{P}$  and  $\mathbf{C}$  are computed as  $b_i \equiv (d_u \tau_{2i} - 1)/(d_u \tau_{2i} + 1)$ ;  $p_i \equiv (1 - b_i)/(1 - a_i)$ ;  $c_i \equiv p_i(b_i - a_i)$  with adaptive-robust tuning their parameters  $\tau_{1i}$ ,  $\tau_{2i}$  and  $k_i$ . Next, the GMC control torque vector  $\mathbf{M}_k^g$  (5) is "re-calculated" into vector  $\mathbf{u}_k^g$  of the GD digital commands using explicit function of the AM distribution between GDs [Matrosov and Somov, 2004].

The GMC is unloaded from accumulated AM by the compensation scheme with digital control of a magnetic actuator [Somov et al., 2021b]. Station-keeping of mini-satellites on sun-synchronous orbits is implemented by electric propulsion units.

## 7 Simulation of the AOCS Operation

First, a computer simulation of an orthodromic scanning survey of two sites with best quality was performed using formation of four mini-satellites weighing 250 kg in sun-synchronous orbits with altitude of 600 km.

The flight time is counted from the moment when any SC passes the ascending node of its orbit. A survey of

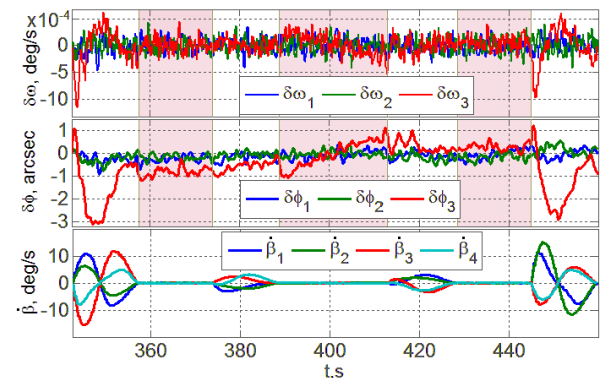


Figure 8. The SC #1 attitude errors and angular rates of the GDs

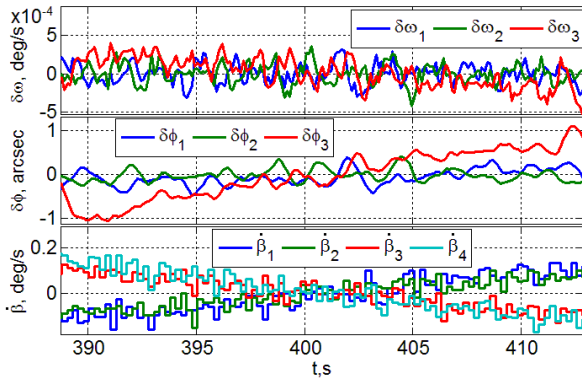


Figure 9. The SC#1 attitude errors on 2nd scan and the GD rates

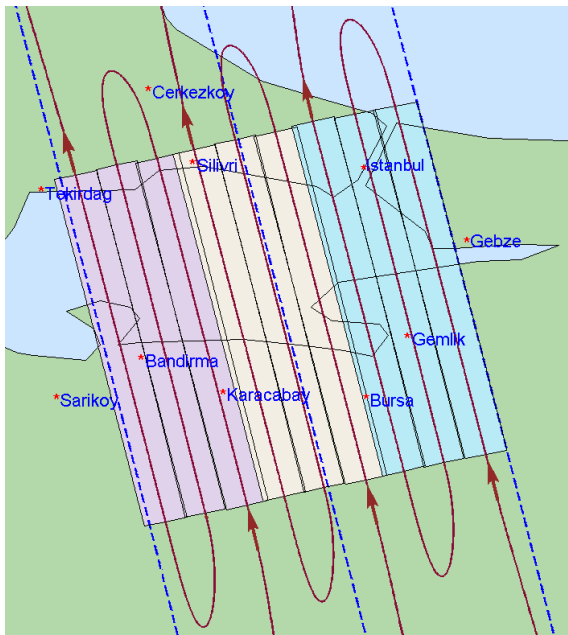


Figure 10. A surveying Istanbul environs and Marmara Sea

the UAE territory (left pair of pink and yellow scans) is performed by SC #1 and SC #2, and when observing the Hormuz Strait (right pair of pink and yellow scans) – by the SC #3 and SC #4, see Fig. 6. In Figures 7 & 8 we represent the guidance law and the orientation errors for the SC #1, and in Fig. 9 – influence of the IMU noise.

Next, we have studied the space surveying of three adjacent Earth sites, each of three scans performed by three mini-satellites, namely left (SC #1), central (SC #2) and right (SC #3) according to the location of their routes in ascending order longitude at geodetic latitude 40 deg, Fig. 10. Here, the accepted location of scans on the Earth surface occurs in a westerly direction, i.e. "right-to-left".

Then the eastern departure of the sets of the observed surface due to the Earth rotation is compensated by the movement to the west when the scans are changed. This option is preferable because it reduces the range of variation and maximum values of the SC roll angles. The guidance law and the orientation errors of mini-satellite #3 are presented in Figs. 11 and 12.

### Conclusions

The navigation and control problems of mini-satellites in formation for Earth areal survey were studied, guidance laws for a scanning survey and results of computer simulation were represented.

An analytical synthesis method has been developed for the spacecraft angular guidance law during areal survey, which is represented by a set of smoothly conjugate vector splines of various degrees.

The important new result was obtained by comparison of the eastward and westward areal survey sequences. In the second variant, the sequence of scans occurs "from right to left" and the eastward drift of the observed terrestrial targets due to the Earth's rotation is partially compensated by the movement to the west when changing scans. Such a sequence of scans is especially preferable for observation satellites from sun-synchronous orbits, since here the maximum values of the roll angles of the mini-satellite are reduced during areal survey.

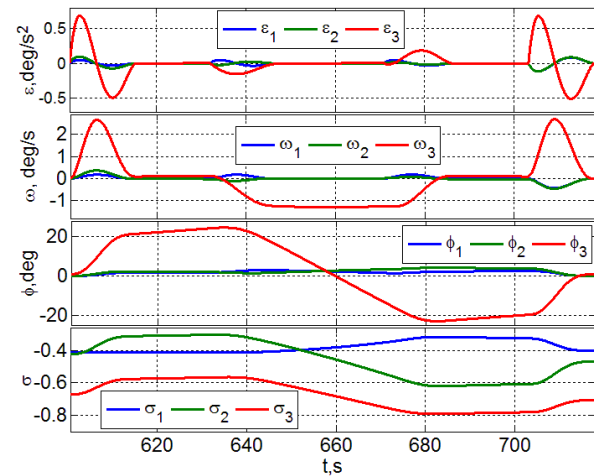


Figure 11. The angular guidance law for mini-satellite #3

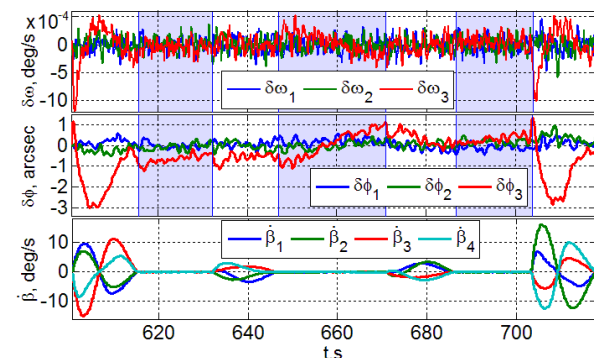


Figure 12. Errors of the SC #3 attitude and the GD angular rates

### References

Aleksandrov, A. and Tikhonov, A. (2018). Rigid body stabilization under time-varying perturbations with zero mean values. *Cybern. Phys.*, 7 (1), pp. 5–10.

- Ballard, A. (1980). Rosette constellations of earth satellites. *IEEE Trans Aerosp Electron Syst*, **16** (5), pp. 656–673.
- Chernov, A. and Chernyavsky, G. (2004). *Orbits of Earth Remote Sensing Satellites*. Radio & Svyaz, Moscow
- Crisp, N., Roberts, P., Romano, F., and et al. (2021). System modelling of very low earth orbit satellites for earth observation. *Acta Astronaut.*, **187**, pp. 475–491.
- Lang, T. (2003). Walker constellations to minimize revisit time in low earth orbit. *Adv. Astronaut. Sci.*, **114**, pp. 1127–1143.
- Lappas, V. and Kostopoulos, V. (2020). A survey on small satellite technologies and space missions for geodetic applications. In *Satellites Missions and Technologies for Geosciences*, chapter 8, pp. 1–22. IntechOpen.
- Matrosov, V. and Somov, Y. (2004). Nonlinear problems of spacecraft fault tolerant control systems. In Sivaram, S., editor, *Nonlinear Problems in Aviation and Aerospace. Vol. 12: Advanced in Dynamics and Control*, pp. 309–331. CRC Press / Taylor & Francis.
- Mozhaev, G. (1989). *Synthesis of Orbital Structures of Satellite Constellations. Group-Theoretic Approach*. Mashinostroyeniye, Moscow.
- Razoumny, Y. (2016). Fundamentals of the route theory for satellite constellation design for earth discontinuous coverage. *Acta Astronaut.*, **128**; **129**, pp. 722–740, 741–758; 447–458, 459–465.
- Rodriguez-Donaire, S. and et al. (2020). Earth observation technologies: low-end-market disruptive innovation. In *Satellites Missions and Technologies for Geosciences*, chapter 7, pp. 1–15. IntechOpen.
- Somov, Y., Butyrin, S., and Somov, S. (2021a). Dynamics of an autonomous spacecraft control system at initial transition to a tracking mode. *Cybern. Phys.*, **10** (3), pp. 185–190.
- Somov, Y., Butyrin, S., Somov, S., and Somova, T. (2017). In-flight calibration, alignment and verification of an astroinertial attitude determination system for free-flying robots and land-survey satellites. In *4th IEEE Workshop on Metrology for Aerospace*, Padua, pp. 474–478.
- Somov, Y., Butyrin, S., and Somova, T. (2019). Guidance, navigation and control of a surveying satellite when an area imagery for disaster management. *Math. Eng. Sci. Aerosp.*, **10** (3), pp. 433–449.
- Somov, Y., Butyrin, S., and Somova, T. (2022). Physical hysteresis of the piezoelectric drive in precise image velocity stabilization system built into the earth observing orbit telescope. *Cybern. Phys.*, **11** (3), pp. 157–164.
- Somov, Y., Butyrin, S., Somova, T., and Somov, S. (2018). In-flight verification of attitude control system for a land-survey satellite at a final of its manufacturing. *IFAC PapersOnLine*, **51** (30), pp. 66–71.
- Somov, Y., Butyrin, S., Somova, T., and Somov, S. (2021b). Health checking autonomous attitude control system of Earth-observing miniature satellite in initial orientation modes. *IEEE Journal on Miniaturization for Air and Space Systems*, **2** (2), pp. 51–58.
- Somova, T. (2016). Attitude guidance and control, simulation and animation of a land-survey satellite motion. *Journal of Aeronautics and Space Technologies*, **9** (2), pp. 35–45.
- Ulybyshev, S. (2016). The use of sun-synchronous orbits for a real-time global coverage satellite. *Cosmic Res*, **54** (6), pp. 445–451.
- Ulybyshev, S. and Lysenko, A. (2019). Design of satellite constellations for operational global monitoring with a daily repeat of flight track. *Cosmic Res*, **57** (3), pp. 204–212.
- Walker, J. (1984). Satellite constellations. *Journal of the British Interplanetary Society*, **24**, pp. 369–384.